Available online at www.sciencedirect.com
ScienceDirect
Proceedings of the Combustion Institute 31 (2007) 2117–2124
Proceedings of the Combustion Institute
www.elsevier.com/locate/proci

Flame behavior in heated porous sand bed

S.G. Kim [a], T. Yokomori [a], N.I. Kim [b], S. Kumar [a], S. Maruyama [a], K. Maruta [a,*]

[a] Institute of Fluid Science, Tohoku University, 2-1-1 Katahira, Aoba-Ku, Sendai 980-8577, Japan
[b] Department of Mechanical Engineering, Chung-Ang University, Republic of Korea

Abstract

This paper reports experimental and numerical investigations on the combustion characteristics of a lean methane–air mixture in a heated porous sand bed. The porous bed consisted of sand (SiO_2) particles with a mean particle diameter of 0.56 mm. The horizontally placed quartz tube was heated externally to initiate the combustion reaction in the porous bed combustor. The stabilized flame location curve as a function of averaged mixture velocity was obtained for various equivalence ratios. Contrary to the earlier finding of a C-shape flame stabilization behavior, a new S-shape behavior was observed in the present study. This can be divided into three regimes: high, moderate, and low velocity regimes. In the low velocity regime, flame with very weak luminosity was confirmed and the stabilized flame location moved downstream with the increase of the mixture velocity. For the moderate velocity regime, a stable flat flame was observed and the flame location moved upstream with the increase of the mixture velocity. An oscillatory flame behavior was observed in the high velocity regime. In this oscillatory mode, the flame front oscillated with a characteristic time period of the order on 1 h and increased with the increase of the mixture velocity. In order to further understand these experimental results, one-dimensional computational studies with detailed chemistry and heat transfer mechanisms were carried out. The computational results were in good agreement with experimental observations. The computations showed that solid-to-solid radiation played a significant role in the flame stabilized location. From the examination of the flame structure, it was found that the flame behavior in the low velocity regime was similar to that of the flameless combustion mode.

Keywords: Porous bed combustion; Oscillatory flame; Flameless combustion; Solid-to-solid radiation

1. Introduction

Fluidized bed combustion systems have been utilized for industrial incinerators because of their inherent advantage of low NO_x emissions and higher combustion efficiency [1,2]. These systems use waste and low calorific value fuels such as sewage sludge or livestock waste as primary fuel. Since such waste contains large amounts of water and incombustible material, it is difficult to sustain stable combustion. Due to this reason, gaseous fuels such as methane or propane are introduced to enhance the combustion stability in a fluidized bed. The usage of an external electric heater is also proposed to improve the combustion stability in such incinerators. The combustion

* Corresponding author. Fax: +81 22 217 5311.
E-mail address: maruta@ifs.tohoku.ac.jp (K. Maruta).

1540-7489/$ - see front matter © 2006 The Combustion Institute. Published by Elsevier Inc. All rights reserved.
doi:10.1016/j.proci.2006.08.070

Nomenclature

A	Cross-sectional area of the combustion tube	$\dot{\omega}_k$	Molar rate of production of kth species
A_t	Outer surface area of tube/unit length	ε	Porosity
c_p	Specific heat of gas	ρ	Density
D_p	Particle diameter of spheres	ϕ	Equivalence ratio
h_{gs}	Volumetric heat transfer coefficient between gas and solid	σ	Stefan–Boltzmann constant
k_r	Radiative thermal conductivity	*Nondimensional*	
λ	Thermal conductivity	*Nu*	Nusselt number
$\dot{q}_r$	Radiative heat flux in axial direction	*Pr*	Prandtl number
T	Temperature	*Re*	Reynolds number
T_h	Heater temperature		
U	Mixture velocity	*Subscripts*	
Y_k	Mass fraction of kth species	g	Gas phase
V_k	Diffusional velocity of kth species	s	Solid phase
W_k	Molecular weight of kth species	k	Species index

phenomenon in a fluidized bed combustor is intrinsically correlated with both the gas reaction in bubbles and the gas reaction in the condensed phase [3]. Although, the gas reaction in bubbles can be treated based on typical gas combustion phenomena, the gas reaction in the condensed phase of the fluidized bed is remarkably different from that of ordinary gas combustion. To understand the gas reaction in the condensed phase, porous media is an appropriate choice due to its simplicity compared to the complicated combustion process in fluidized bed combustion systems.

Combustion in porous media is also known as filtration gas combustion and has been investigated by many researchers [4–10] to understand the combustion characteristics in the condensed phase. Katani et al. [11] have studied the stability limits and combustion characteristics in a bundled ceramic tube burner. They observed that the flame is located in the downstream or upstream region or within the combustion tube depending on the flow rates and equivalence ratios. Similar combustion regimes have been observed by Babkin et al. [12–14]. They observed two different velocity regimes for the stabilized flame location in a porous bed: the low velocity regime (LVR) and the high velocity regime (HVR). In the low velocity regime, the reaction zone and temperature profiles in gas and solid phases propagate as a united structure with a velocity on the order on 1 cm/s. In the high velocity regime, the gas combustion zone moves almost independently of the solid temperature profile. In between these two regimes, transient flame propagation was observed. However, the behavior of stabilized flame within the porous media was not fully investigated.

Various researchers [15–17] have emphasized the importance of various heat transfer mechanism, especially the role of solid-to-solid radiation. Chen et al. [15] have reported that the solid-to-solid radiation used to preheat an unburned mixture leads to an increase of burning velocity and reduced flame thickness. Further study of the importance of solid-to-solid radiation has been conducted by Yoshizawa et al. [16]. They simulated combustion in porous media by using three different sections of the burner and concluded that solid-to-solid radiation plays an important role in excess enthalpy burning. In spite of the fact that the earlier works investigated the effect of solid-to-solid radiation, the effect of solid-to-solid radiation on the stabilized flame location remains unclear.

In the present study, the combustion characteristics of a fuel-lean methane–air mixture in a heated porous sand bed were investigated both experimentally and numerically. The different flame stabilization regimes were classified into appropriate categories and the flame behaviors in these regimes were discussed. The effect of solid radiation on the flame stabilization was also examined by using different models with and without solid-to-solid radiation heat transfer. The flame behavior was examined based on analysis of the flame structure in each corresponding regime.

2. Experimental setup

A schematic diagram of the experimental apparatus is shown in Fig. 1. The sand was packed in a quartz tube as a porous material. The thermal conductivity and the permeability (for the single phase flow) of the sand bed were 2.7×10^{-1} W/mK and 2.0×10^{-7} cm^2, respectively [18]. The mean diameter of SiO_2 sand particle was

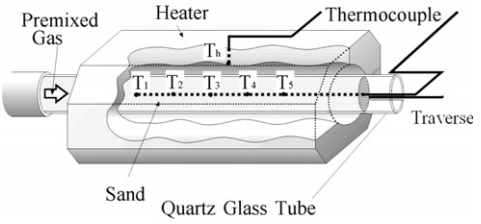

Fig. 1. Experimental setup.

0.56 mm, which was determined by sieve analysis. The combustion tube had an inner diameter of 27 mm and a length of 450 mm. An external electric heater was used to heat the porous sand bed. The heater was located 150 mm downstream of the point where the mixture entered the porous sand bed. The initial temperature distribution of the porous sand bed is shown in Fig. 2. The highest temperature in the porous sand bed was maintained at around 1330 K.

Lean methane–air mixtures with equivalence ratios of 0.1 and 0.5 were supplied to the porous sand bed. Electric mass flow controllers were used to control the mass flow rates of both methane and air. The mixture velocity was defined as $U = \dot{m}/(\rho_0 A_g)$, where $\dot{m}$, ρ, and A_g are mass flow rate, density at room temperature, and effective area of gas, respectively. The effective area of gas was defined as $A_g = A\varepsilon$, where A and ε are the cross-sectional area of the quartz tube and the porosity of the bed. Additionally, the effective area of solid was $A_s = A(1-\varepsilon)$. The porosity was defined as the ratio of free volume to the total bed volume and estimated to be 0.25 by assuming a homogeneous porous bed consisting of spheres with a mean diameter of 0.56 mm.

Five thermocouples (K-type, 500 μm, and sheath type) were arranged along the centerline of the porous sand bed with 50 mm intervals from the downstream side of combustor as shown in Fig. 1. To determine the flame location in the porous bed, one thermocouple was traversed through the porous sand bed with the help of a micrometer traverse (minimum resolution of 0.05 mm for the flame front measurement in the present study) and the temperature distribution was obtained. The flame was assumed to be located at a point where peak temperature was observed. Measurement of the stabilized flame location was conducted under the steady state conditions. The system was confirmed to be in steady state when the value of temperature fluctuation remained within 3 K during 1 h.

3. Experimental results

The stabilized flame location was measured by tracing the peak temperature position by traversing a thermocouple in the axial direction. Variation of the stabilized flame location with mixture velocity for different equivalence ratios ($\phi = 0.5$ and 0.1) is shown in Fig. 3. It was difficult to determine the flame position at very low mixture velocities due to very low heat release rate and the absence of an explicit temperature peak. Therefore, a different criterion was used to determine the flame position at low mixture velocities. The flame front was assumed to be located at a position where the difference between the initial (without mixture flow) and final (with mixture flow) temperature profiles of the porous bed was observed to be maximum. Figure 3 shows that the stabilized flame location exhibits S-shaped behavior for $\phi = 0.5$. This S-shaped behavior can be divided into three regimes, namely low, moderate, and high velocity regimes. In the low and high velocity regimes, the flame front moves downstream with the increase of the mixture velocity. Contrary to this tendency in the low and high velocity regimes, the opposite tendency of flame front movement in the upstream direction is observed for the moderate velocity regime. This is due to strong heat recirculation through the porous media [17]. The increase of the

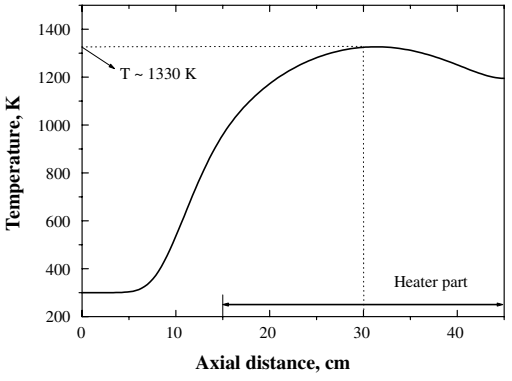

Fig. 2. Initial temperature profile of porous bed burner.

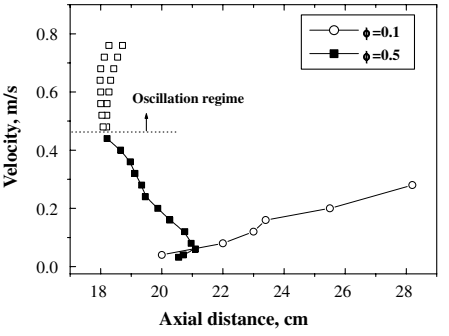

Fig. 3. Experimental result of variation of the stabilized flame location with mixture velocity.

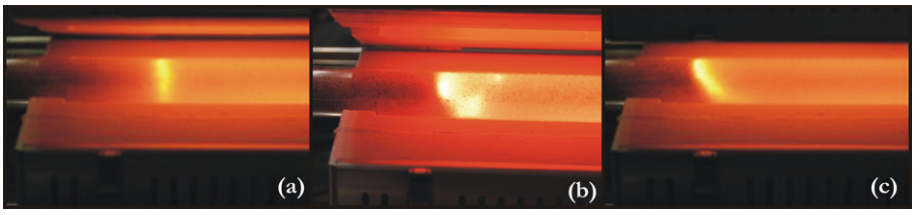

Fig. 4. Direct photographs of flame front at $\phi = 0.5$ (a) $U = 0.24$ m/s, (b) $U = 0.48$ m/s, and (c) $U = 0.56$ m/s.

incoming enthalpy with the increase of the mixture flow rate increases the effect of heat recirculation up to a certain value of the mixture flow rate, which results in a flame shifts in the upstream direction. However, with a further increase in the mixture flow rate, the residence time decreases and this becomes dominant. Since the amount of the incoming enthalpy is very small for $\phi = 0.1$, such S-shaped behavior was not observed and the flame front shifts monotonically in the downstream direction with an increase of the mixture velocity. For $\phi = 0.5$, oscillatory flame behavior was observed in the high velocity regime and for mixture velocity greater than 0.48 m/s. The flame oscillated between two axial locations which were measured by tracing the position of the peak temperature. The approximate variation of the flame location in the axial direction is shown in Fig. 3 with open square symbols. A detailed description of this oscillatory behavior will be presented later.

Figure 4 shows flame front photographs for the moderate and high velocity regimes. No image for the low velocity regime is shown because luminosity from the reaction zone in this regime was much weaker than the radiative emission from the sand bed. Figure 4a shows the flame front in the moderate velocity regime ($\phi = 0.5$, $U = 0.24$ m/s). The flame front is nearly flat and it is stable in this regime. On the other hand, an inclined flame front is observed in the high velocity regime ($\phi = 0.5$, $U = 0.56$ m/s) as shown in Fig. 4c. Between these two regimes, an interesting feature of the flame front is observed where it breaks down into two parts: top and bottom as shown in Fig. 4b. The collapse of the flame front may be related to the transition of the combustion mode from a stable to an oscillatory regime.

Figure 5 shows variation of the oscillatory time periods with the mixture velocity. It is interesting to note that the oscillatory time periods are on the order of an hour and gradually increase with mixture velocity. This oscillatory flame behavior was confirmed to be independent of apparatus related factors since small fluctuations in heater temperature (within ±0.4%) have no correlation with temperature histories in the porous bed. Although many researchers [19–21] have reported the existence of oscillatory flame behavior in porous beds, a long time period (on the order of an hour) of

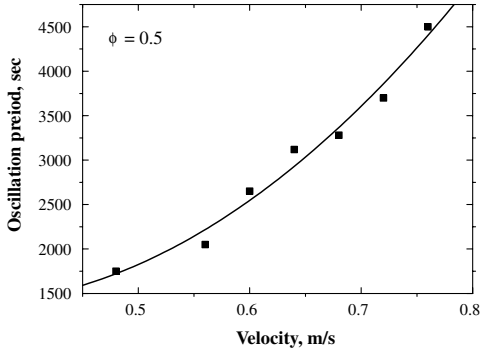

Fig. 5. Experimental results of variation of oscillation period with mixture velocity.

flame oscillations has not been reported in the literature. This oscillatory behavior with a long time period is probably related to the inclined flame front in the porous sand bed. Since the value of Gr/Re^2 based on the pore size and heater temperature as an ambient of the porous bed is very small ($\ll 1$) in the present system, buoyancy may not play a significant role in these instabilities such as inclined flame front and oscillatory behavior. Thus, we suspect that the cause of these instabilities may be related to the diffusive-thermal instability, including large radiative heat transfer. To clarify this, further studies are being carried out on these flame oscillations.

4. Computation model

In order to further understand the experimental results, one-dimensional computational studies were carried out by using a PREMIX [22]-based code. The experimental geometry and initial temperature profile shown in Fig. 2 were used for the present calculations. All the calculations were conducted for methane–air mixtures. Energy equations for the solid and gas phases are as follows:

$$\dot{m}\frac{\mathrm{d}T_\mathrm{g}}{\mathrm{d}x} - \frac{1}{c_\mathrm{p}}\frac{\partial}{\partial x}\left(\lambda A_\mathrm{g}\frac{\mathrm{d}T_\mathrm{g}}{\mathrm{d}x}\right) + \frac{A_\mathrm{g}}{c_\mathrm{p}}\sum_{k=1}^{K}\rho Y_k V_k c_{\mathrm{p}k}\frac{\mathrm{d}T_\mathrm{g}}{\mathrm{d}x}$$

$$+\frac{A_g}{c_p}\sum_{k=1}^{K}\dot{\omega}_k h_k W_k + \frac{A_g}{c_p}h_{gs}(T_g - T_s) = 0 \quad \text{(GasPhase)}$$

$$-\frac{\partial}{\partial x}\left(\lambda_s A_s \frac{dT_s}{dx}\right) + A_s h_{gs}(T_s - T_g) - A_s\frac{dq_r}{dx} + \dot{Q} = 0 \quad \text{(SolidPhase)}$$

Here,

$$q_r = -k_r\frac{dT_s}{dx}, \quad k_r = \frac{16\sigma T_s^3}{3\beta}, \quad \dot{Q} = A_t\sigma(T_s^4 - T_h^4)$$

The effect of solid conduction, convective heat transfer, and radiative heat transfer in the porous sand bed was considered. Gas phase thermochemical and transport properties were obtained from the Chemkin [23] and Tranfit [24] packages. The C-1 chemical kinetics mechanism [25] was used. The solid-to-solid radiation, hereafter described as solid radiation, was approximated using optically thick approximation [26]. The radiative properties such as albedo, emissivity, and extinction coefficient were assumed to be unity. The heat transfer coefficient for forced convection through the packed bed [27] was calculated by using the following relation:

$$Nu = \frac{h_{gs}D_p}{\lambda(1-\varepsilon)\psi} = 2.19(RePr)^{1/3}$$

Here, D_p, λ, and ε are particle diameter of spheres, thermal conductivity of gas, and porosity, respectively. The quantity ψ is a particle shape factor. Thermal conductivity of solid phase, λ_s was assumed to be constant [28]. Computations for flame behavior such as the flame stabilization characteristic were conducted to interpret the observed experimental results in detail. In addition, the effect of solid radiation on the stabilized flame location was examined by comparing the two computational models, namely the case with solid radiation (Model I) and that without solid radiation (Model II).

5. Computational results and discussion

5.1. Stabilized flame location

In order to understand the various combustion characteristics of gas combustion such as flame stabilization and its structure in a porous sand bed, computational studies were carried out. Figure 6 shows the computational results of variations of the stabilized flame location with mixture velocity at $\phi = 0.1$ and $\phi = 0.5$. For purpose of comparison, the experimental results are also presented in Fig. 6. Computational results without solid radiation predicts S-shaped behavior for the stabilized flame location at $\phi = 0.1$, while those with solid radiation predict a monotonic dependence on the stabilized flame location, which is similar to the experimental results for $\phi = 0.1$. On the other hand, there was a limitation point for the steady solution in the $\phi = 0.5$ condition. The present code could not predict the steady solution beyond $U = 0.372$ m/s for the case with solid radiation and $U = 0.167$ m/s for that without solid radiation. This may indicate the existence of unstable solutions such as oscillatory behavior beyond these velocity conditions. Both computational results with and without solid radiation show a trend similar to that of the experimental results. It is also seen that the prediction results with solid radiation (Model I) are in better agreement with the experimental results than the predictions from without solid radiation (Model II) qualitatively.

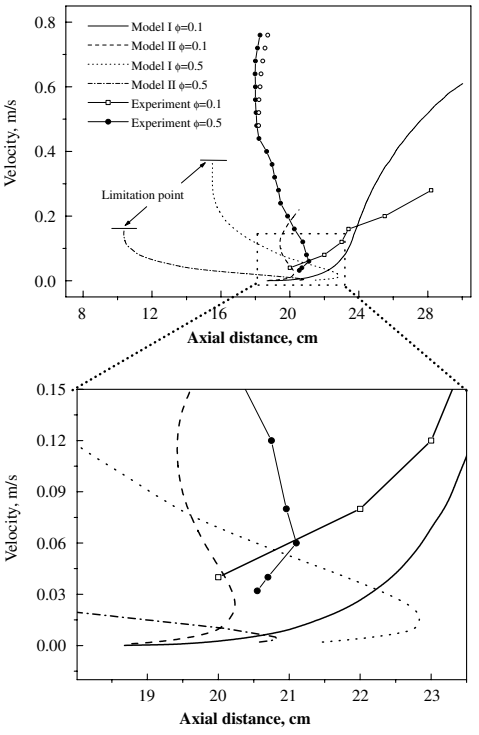

Fig. 6. Computational results of variation of flame location with mixture velocity. Here, Model I includes solid radiation term and Model II is without solid radiation term.

5.2. Flame structures

The flame structures in the moderate and high velocity regimes were similar to a conventional premix flame. The typical flame structure in the high velocity regime is shown in Fig. 7a, which shows a distinct temperature peak along with a

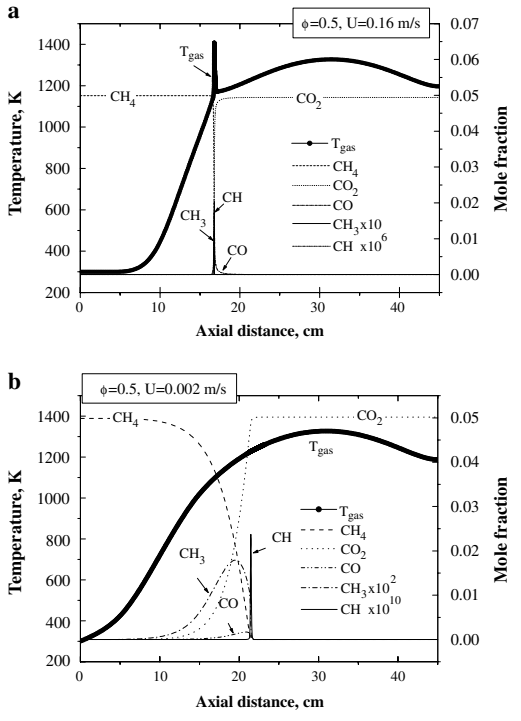

Fig. 7. Computational result of the flame structure (a) for $\phi = 0.5$, $U = 0.16$ m/s, (b) for $\phi = 0.5$, $U = 0.002$ m/s with solid radiation.

thin reaction zone. The methane is rapidly consumed near the reaction zone and the other intermediate chemical species such as CH, CH_3, and CO are generated within the thin reaction zone. However, the flame structure in the low velocity regime is remarkably different from that in the high velocity regime, as shown in Fig. 7b. Therefore, it is important to understand the flame structure in the low velocity regime. A remarkable feature of the flame structure in the low velocity regime is the absence of the peak temperature in the reaction zone and existence of a wide reaction zone as indicated by the width of CH_3, CH, and other species profiles in Fig. 7b. Since no peak temperature in the reaction zone was observed, the location of the maximum CH peak in the calculation was considered to be the stabilized flame location. Despite the absence of a temperature peak in the reaction zone, combustion reaction was completed as shown in Fig. 7b. CH_4 is gradually consumed throughout the reaction zone. The intermediate species such as CH_3 and CO are generated over a wider zone, which is approximately 100 mm. Similar combustion phenomena with a wider reaction zone are observed in mild combustion or flameless combustion systems [29–31]. This type of flameless combustion behavior in the low velocity regime for porous bed combustion has not been reported earlier.

5.3. Effect of solid radiation on stabilized flame location

Figure 8 shows the variation of the peak temperature in the reaction zone. The peak temperature increases rapidly up to a mixture velocity of around 0.025 m/s, and beyond that, it increases gently with the increase of mixture velocity. Both computational results showed the same trend. On the other hand, it is seen that the difference of peak temperature of these computation results is very small (~15 K at maximum).

Figure 9 shows a comparison of the computational flame structure at $\phi = 0.5$ and $U = 0.16$ m/s with and without solid radiation. As shown in Fig. 9, the stabilized flame location is remarkably different for these two cases, even though the results were obtained at the same equivalence ratio and velocity condition. Both computations predicted a difference of peak temperature of only

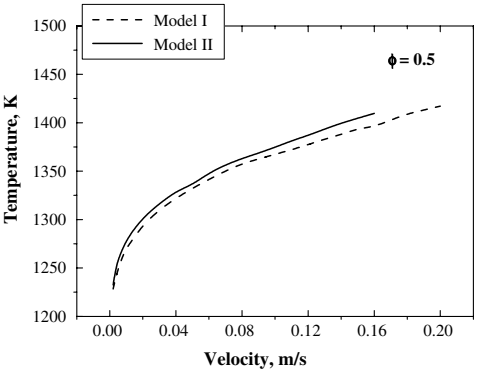

Fig. 8. Computational results of variation of peak flame temperature with mixture velocity for $\phi = 0.5$. Model I includes solid radiation term and Model II is without solid radiation term.

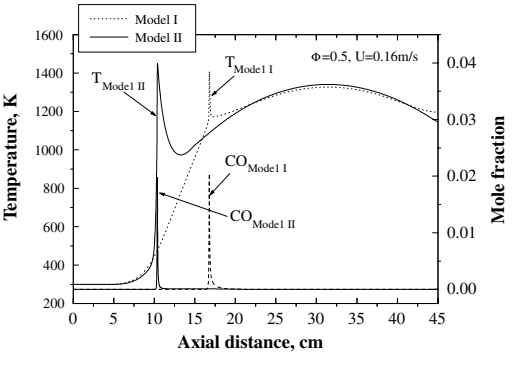

Fig. 9. Computational result of comparison of flame structure in high velocity regime for $\phi = 0.5$, $U = 0.16$ m/s. Model I includes solid radiation term and Model II is without solid radiation term.

15 K in the reaction zone as shown in Fig. 8. However, the high temperature zone generated by chemical reaction for the case of without solid radiation is much broader than that in the case with solid radiation as shown in Fig. 9. In addition, the temperature distribution in the axial direction for the case with solid radiation is flatter than the temperature distribution for the case without solid radiation. This indicates that the heat loss from the high temperature zone to the lower temperature zone upstream and downstream of the reaction zone is much higher for the case with solid radiation compared with that for the case without solid radiation. Therefore, the total heat recirculation rate is much larger for the case without solid radiation when compared with the case with solid radiation. Therefore, the flame front is stabilized in the upstream region in the case without solid radiation.

6. Conclusions

Combustion characteristics of a lean methane–air mixture in a heated porous sand bed were investigated both experimentally and numerically. It was observed that the stabilized flame location exhibits S-shaped behavior for $\phi = 0.5$ with mixture velocity. This S-shaped behavior can be categorized into three regimes, namely high, moderate, and low velocity regimes. For the moderate velocity regime, a stable flat flame was observed. Oscillatory behavior was observed in the high velocity regime. The flame front oscillated with a characteristic time period on the order of 1h and increased with the increase of the mixture velocity. An inclined flame front was observed in such conditions. A simple monotonous dependence of flame location on mixture velocity was observed for $\phi = 0.1$. The effect of solid radiation on the flame behavior was examined through computational studies. It was clarified that solid radiation plays a significant role in flame stabilization. From the examination of the flame structure, it was found that the flame behavior in the low velocity regime was similar to that in the flameless combustion mode.

References

[1] M. Pilawska, C.J. Butler, A.N. Hayhurst, D.R. Chadeesingh, *Combust. Flame* 127 (2001) 2181–2193.

[2] W. Wu, A.P. Dellenback, P.K. Agarwal, H.W. Haynes Jr., *Combust. Flame* 140 (2005) 204–221.

[3] J. Baron, E.M. Bulewicz, W. Zukowski, *Combust. Flame* 128 (2002) 410–421.

[4] S.B. Sathe, R.E. Peck, T.W. Tong, *Combust. Sci. Technol.* 70 (4–6) (1990) 93–109.

[5] J.G. Hoffmann, R. Echigo, H. Yoshida, S. Tada, *Combust. Flame* 111 (1997) 32–46.

[6] R. Mital, J.P. Gore, R. Viskanta, *Combust. Flame* 111 (1997) 175–184.

[7] T. Yokomori, S.G. Kim, N.I. Kim, T. Kataoka, S. Maruyama, K. Maruta, 5th Asia-Pacific Conference on Combustion, Australia (2005) 97–100.

[8] S. Zhdanok, Lawrence A. Kennedy, G. Koester, *Combust. Flame* 100 (1995) 221–231.

[9] R.M. Henneke, J.L. Ellzey, *Combust. Flame* 117 (1999) 832–840.

[10] T. Takeno, K. Sato, *Combust. Sci. Technol.* 20 (1–2) (1979) 73–84.

[11] Y. Katani, H.F. Behahani, T. Kakeno, *Proc. Combust. Inst.* (1985) 2025–2033.

[12] V.S. Babkin, V.A. Bunev, A.A. Korzhavin, in: L.N. Stesik (Ed.), *Combustion of Gases and Natural Fuels*, OICHF, CHernogolovka, 1980, p. 87.

[13] V.S. Babkin, A.A. Korzhavin, V.A. Bunev, *Combust. Flame* 87 (1991) 182–190.

[14] S.S. Minaev, S.I. Potytnyakov, V.S. Babkin, *Comust. Explosion Shock Waves* 30 (1994) 306–310.

[15] Y.K. Chen, R.D. Matthews, J.R. Howell, in: *Radiation, Phase Change Heat Transfer, and Thermal Systems Annual Meeting of ASME*, December 13–18, vol. 81, 1987, pp. 35–41.

[16] Y. Yoshizawa, K. Sassaki, R. Echigo, *Int. J. Heat Mass Transfer* 31 (2) (1988) 311–319.

[17] A.J. Barra, J.L. Ellzey, *Combust. Flame* 137 (2004) 230–241.

[18] D.A. Nield, A. Bejan, *Convection in Porous Media*, second ed., Springer-Verlarg, New York, 1998, p. 5.

[19] A.V. Saveliev, A.L.A. Kennedy, A.A. Fridman, I.K. Puri, *Proc. Combust. Inst.* 26 (1996) 3369–3375.

[20] O.S. Rabinovich, A.V. Fefelov, N.V. Pavlyukevich, *Proc. Combust. Inst.* 26 (1996) 3383–3389.

[21] G.A. Fateev, O.S. Rabinovich, M.A. Silenkov, *Proc. Combust. Inst.* 27 (1998).

[22] R.J. Kee, J.F. Grcar, M.D. Smooke, J.A. Miller, Sandia National Lab., Report SAND, 1994, 85-8240.

[23] R.J. Kee, G. Dixon-Lewis, J. Warnatz, M.E. Coltrin, J.A. Miller, Sandia National Lab., Report SAND, 1986, 86-8246.

[24] R.J. Kee, F.M. Rupley, J.A. Miller, Sandia National Lab., Report SAND, 1989, 89-8009B.

[25] M.D. Smooke, *J. Comput. Phys.* 48 (1982) 72.

[26] J.P. Holman, J.R. Lioyd, *Radiative Heat Transfer*, first ed., McGraw-Hill, New York, 1990, pp. 485–488.

[27] R.B. Bird, W.E. Stewart, E.N. Lightfoot, *Transport Phenomena*, second ed., John Wiley & Sons, New York, 2002, p. 441.

[28] A.G. Dixson, D.L. Cresswell, *J. AICHE* 25 (1979) 663–676.

[29] J.M. Ahn, C. Eastwood, L. Sitzki, P.D. Ronney, *Proc. Combust. Inst.* 30 (2005) 2463–2472.

[30] K. Maruta, K. Muso, K. Takeda, T. Niioka, *Proc. Combust. Inst.* 28 (2000) 2117–2123.

[31] K. Maruta, T. Kataoka, N.I. Kim, S. Minaev, R. Fursenko, *Proc. Combust. Inst.* 30 (2005) 2429–2436.

Comments

A.N. Hayhurst, University of Cambridge, UK. Combustion in a hot bed of sand is inhibited by the recombination of radicals on the exterior of each sand particle [1]. Because of this, did you vary the size of the sand particles in your experiments or include these heterogeneous effects in your modeling?

Reference

[1] J.S. Dennis, A.N. Hayhurst, I.G. Mackley, *Proc. Combust. Inst.* 19 (1982) 1205–1212.

Reply. We did not vary the size of the sand particles in the present study. Kim et al. [1] showed the homogeneous chemical reactions overcome the effect of radical removal by the surface and flame becomes resistant to quenching when the temperature of the solid wall is above 873 K. Since mean temperature (1330 K) of present experiment is sufficiently higher than the solid temperature (873 K), we did not consider the surface reaction (radical quenching / recombination in the present work.

We did not include the heterogeneous effects into the modeling of chemical reaction in the present computations for the reasons stated above.

Reference

[1] Kyu Tae Kim, Dae Hoon Lee, Sejin Kwon, *Combust. Flame* 146 (2006) 19–28.

●

David Smith, University of Leeds, UK. Following Allan Hayhurst's comment, as an alternative to changing particle size to assess the significance of radical loss on sand surfaces, one might treat the particles with different wash coatings e.g., KCl or B_2O_3. Classic work on the H_2/O_2 system by Baldwin and Walker [1] showed that this can cause very different surface activity.

References

[1] R.R. Baldwin, D.H. Langford, R.W. Walker, *Trans. Farad. Soc.* 65 (1969) 792.
[2] R.R. Baldwin, A.R. Fuller, D. Longthorn, R.W. Walker, *Trans. Farad. Soc. (I)* 70 (1974) 1257.

Reply. The effects of radical recombination and radical quenching are not significant in high temperature (1330 K) for CH_4/air system as shown in Kim et al. ([1] in reply to Hayhurst). Therefore, the effect of radical loss on the sand surfaces can be neglected in the present study. The H_2/O_2 system might be active at lower temperature, since the sticking coefficient of H_2 is much higher than that of CH_4.